Cascade simulation of a Δ isobar propagating in a nucleus

Kim Sneppen and Carl Gaarde
The Niels Bohr Institute, University of Copenhagen, Blegdamsvej 17, Dk-2100 Copenhagen, Denmark
(Received 9 December 1993)

We present a cascade model to study the measurable consequences of Δ isobars inside a nucleus. We compare the outcome of simulations with observed events from charge exchange reactions on a carbon target. We see that the inclusive energy-transfer spectrum shows differences between model and experiment, when free Δ parameters are used. By changing parameters for the Δ in the formation process to better describe the inclusive spectrum, the gross features of the decay pattern including the energy-transfer spectra for each of the observed event classes are reasonably well accounted for.

PACS number(s): 25.60.+v, 25.40.−h, 13.75.−n

I. INTRODUCTION

In the present paper we describe a cascade model to simulate the formation and propagation of a Δ isobar inside a nucleus. The experimental situation we have in mind is 4π detection of reaction products from reactions like [1,2]

$$^3\mathrm{He} + {}^{12}\mathrm{C} \rightarrow {}^3\mathrm{H} + \mathrm{X} + \cdots , \quad (1)$$

$$p + {}^{12}\mathrm{C} \rightarrow n + X + \cdots , \quad (2)$$

where, in addition to the fast forward going ejectile, some protons and/or pions are detected. The purpose is to determine to what extent the reaction channels carry information about the properties of a Δ isobar inside the nuclear medium. The philosophy of the calculation is to include all known properties of the corresponding free particles, and then see whether this is sufficient to reproduce data where the nuclear medium might play a role.

The approach is classical, with particles that either scatter on the target nucleons, or, between scatterings, move classically in the target mean field. The only quantum effects taken into account are the Fermi motion and the Pauli blocking of the nucleons involved.

Before describing the classical cascade model we stress that such an approach ignores (A) correlations between subsequent events, even within very short distances (e.g., within the "radius" of a nucleon and (B) quantum interference effects. Thus if a particle, here the Δ, has several decay possibilities, then the total decay probability (per unit time) is given as the simple sum of the decay probabilities.

In addition to these fundamental limitations of validity we simplify the cascade procedure by (C) taking all two-particle interactions (collisions) as pointlike in space, (D) describing the target nucleus as a spherical homogeneous distribution of uncorrelated nucleons, and (E) taking the Pauli blocking in a local Thomas-Fermi approximation.

In the literature there are many examples of the use of cascade models. Cugnon *et al.* [3] have recently examined Δ and pion formation in proton and heavy ion induced reactions in such a intranuclear cascade model, but in most cases the available data are not specific enough to really demonstrate the limitations in the approach. Nucleus-nucleus collisions have also been described by transport equations like the Boltzmann-Uehling-Uhlenback (BUU) approximation [4,5]. Recent data from heavy ion collisions in the GeV/nucleon region have been analyzed in this model [6,7]. The present paper deals with the much simpler case of the formation and decay of a single Δ, but on the other hand leaning on much more detailed data.

II. THE MODEL

We now describe the approach in detail. A simplification in the simulation is that we only consider events where the projectile has interacted once with a target nucleon; i.e., we assume that one Δ isobar is formed. Given target, projectile, and beam energy a Monte Carlo cascade calculation is performed in a series of steps.

(1a) A spherical distribution of the A_0 target nucleons is generated. We use a three-parameter Fermi distribution

$$\rho(r) = A_0 \frac{\rho_0}{\{1 + \exp[(r-c)/z]\}^\gamma}, \quad (3)$$

where c, z, and γ are chosen to fit the measured density distributions.[1] The density profile of protons is approximated to be proportional to that of neutrons. Given $\rho(r)$ we calculate a density dependent nuclear mean field $V(r) = V(\rho(r)) = c_1\rho^{7/6} - c_2\rho$ [5] from a standard parametrization of the nuclear equation of state. Furthermore we include the electric forces calculated from the charge distribution.

(1b) A spatial distribution of the initially formed Δ's is calculated with an assumption of straight line trajectory of projectile protons (see the Appendix). As mentioned

[1] For ^{12}C we use ρ_0=0.184 fm^{-3}, z = 0.578 fm, and γ = 1.36.

in the Appendix there may be some ambiguity in how to model the projectile nucleus, in particular whether one should consider it as consisting of three independent pointlike particles (model A) or whether the extension of the projectile should be modeled only as a finite range of the interaction (model B). The two models do however give the same Δ distribution, but in the Appendix we have for completeness described both extremes. In Fig. 1 we show the distribution of initially formed Δ's in a carbon target. For comparison we in the same figure show, with shaded areas, the density profile of the target and the ^{3}He projectile.

(2) A number of sampled events is chosen, typically to be of the order of 10^5.

(3) For an event we select randomly a creation point for the Δ isobar formed according to the distribution calculated in (1b). We then perform the collision between the projectile and a nucleon in that point, with the motion of the nucleon randomly selected from the local Fermi distribution. Including the form factor for the $N(^3\mathrm{He},t)\Delta$ reaction, the cross section for Δ formation has the form [8]

$$\frac{d\sigma}{dt} = \frac{d\sigma}{dt}(NN \to N\Delta)\mathrm{FF}^2(t) = \frac{d\sigma}{dt}(NN \to N\Delta)\left(\frac{2}{3}\mathrm{FF}_T^2(t) + \frac{1}{3}\mathrm{FF}_L^2(t)\right), \tag{4}$$

with the elementary cross section expressed in terms of the invariant flux in the denominator [9]:

$$\frac{d\sigma}{dt}(NN \to N\Delta) = \frac{k(I)g(t)}{(p_1p_2)^2 - (m_1m_2)^2}. \tag{5}$$

Here $-t$ is the four-momentum transfer (squared) and p_1 and p_2 the four-momenta for the nucleons involved in the NN collision. The isospin dependence is given by $k(I)$ (products of isospin Clebsch-Gordan coefficients) and the ^{3}He-t form factor (FF^2) is written as a sum of a transverse and longitudinal contribution. We have used the fact that $p^2\frac{d\sigma}{dt}(t)$ (p is a three-momentum) to a good approximation is independent of energy and have parametrized $g(t)$ to fit the observed t dependence [10]. Selecting t according to the above distribution and selecting the mass M of the Δ from a Breit-Wigner distribution

$$P(M) = \frac{\Gamma(M)}{(M^2 - M_\Delta^2)^2 + M_\Delta^2\Gamma^2(M)}, \tag{6}$$

we have formed a Δ isobar with all kinematic characteristics. Here M_Δ, denoting the mass of the Δ, takes the value 1232 MeV for a free Δ. Notice that the width of the Δ depends on its mass, reflecting the size of the available phase space for the (free) decay into an on-shell pion with mass $m_{\pi^*} = m_\pi = 140$ MeV and a nucleon with mass $m_n = 938$ MeV [9]:

$$\Gamma(M) = \Gamma_0\left(\frac{p_\pi(M)}{p_\pi(M_\Delta)}\right)^3\frac{p_\pi(M_\Delta)^2 + (200\ \mathrm{MeV/c})^2}{p_\pi(M)^2 + (200\ \mathrm{MeV/c})^2}, \quad p_\pi(M) = \frac{(M^2 - m_n^2 - m_{\pi^*}^2)^2}{4M^2} - m_n^2, \tag{7}$$

where the free width $\Gamma_0 = 120$ MeV. Notice that the parameters $(M_\Delta, \Gamma_0, m_{\pi^*})$ of the Δ might be different inside the nuclear medium (at least some broadening of the formed Δ's are expected in order to be consistent with the additional decay possibility $N + \Delta \to N + N$). Before proceeding we check whether a Δ with the chosen mass could be formed with the given four-momentum transfer. If this was not possible we repeat step (3) until an acceptable Δ is formed. Thus the effective cross section for formation of a Δ isobar is

$$\frac{d\sigma}{dt}(NN \to N\Delta) = \frac{k(I)g(t)}{(p_1p_2)^2 - (m_1m_2)^2}\left(\frac{\int_{m_n+m_{\pi^*}}^{m(t)} dM\ P(M)}{\int_{m_n+m_{\pi^*}}^{\infty} dM\ P(M)}\right), \tag{8}$$

from which the total cross section for Δ formation can be found.[2] The charge of the Δ is chosen from the isospin of the involved nucleons with probabilities given by the Clebsch-Gordan coefficients.

(4a) The propagation of the Δ is followed in the attractive nuclear mean field, allowing for the following two decay possibilities:

$$\Delta \to \text{nucleon} + \text{pion} \tag{9}$$

and

$$\Delta + \text{nucleon} \to \text{nucleon} + \text{nucleon}, \tag{10}$$

where the probability for each channel is given respectively by the free Δ decay width $\Gamma(M)$ and by the product of $\rho(r)$ with the inverse cross section for two nucleons forming a Δ. Although the Δ isobar does not correspond to a stable state, we will assume that the cross section for Δ absorption is connected to the cross section for Δ

[2]To test the cross sections in step (3) we have calculated total cross sections of the elementary reactions $p(^3\mathrm{He},t)\Delta^{++}$ at 2 GeV and $p(p,n)\Delta^{++}$ at 800 MeV. Furthermore, as many of the Δ's formed are close to threshold we have checked that the procedure for choosing t and M does in fact reproduce the experimental cross section for the $p(p,n)\Delta^{++}$ reaction around the threshold.

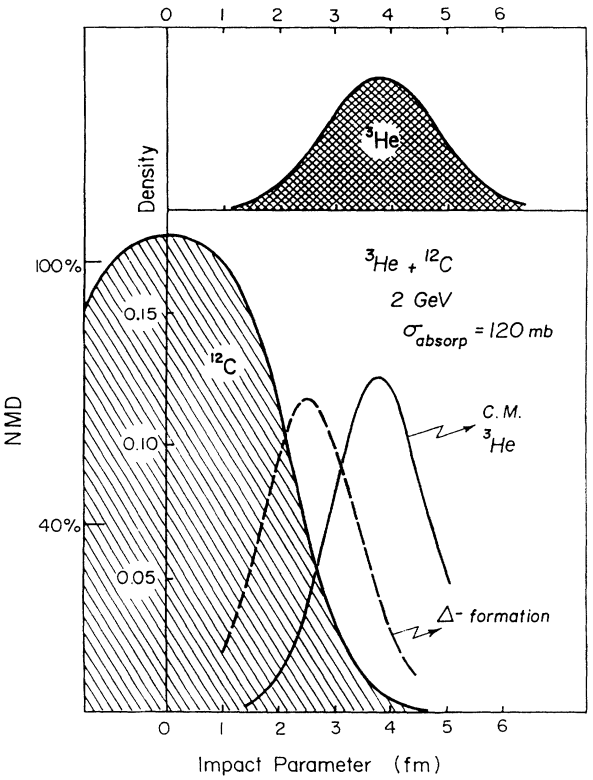

FIG. 1. Delta formation in a carbon nucleus bombarded with a ^{3}He beam of 2 GeV. The dashed curve shows where the initial Δ is formed, the solid curve the distribution of impact parameters of the c.m. of the ejectile. Everything is calculated with straight line trajectories and using the density distributions of the carbon and helium nuclei, as shown by the shaded regions. The projectile distribution is shown corresponding to the most probable impact parameter. Due to the finite extension of the projectile, the Δ's are typically formed deeper inside the target than given by the projectile c.m. trajectory.

formation by detailed balance [11]. For example, for the $n\Delta^{++} \to pp$ channel we use the cross section

$$\frac{d\sigma}{dt}(n\Delta^{++} \to pp) = \frac{1}{4} \frac{g_{n\Delta++}(t)}{(p_n p_\Delta)^2 - (m_n m_\Delta)^2}, \quad (11)$$

where $g_{n\Delta++}(t) = k(I)\, g(t)$ is the experimentally known four-momentum dependent cross section for $pp \to n\Delta^{++}$ and where the factor $\frac{1}{4}$ takes into account a factor $\frac{1}{2}$ for the additional spin channels of the Δ and a factor $\frac{1}{2}$ due to identity of the two protons. As the experimentally measured process we compare to, $pp \to n\Delta^{++}$, has fixed total isospin there is no additional counting for difference in isospin degrees of freedom.[3] We note that all nucleons involved are chosen randomly from the local Fermi sea, and that all nucleonic products are checked for Pauli blocking. In case of blocking the corresponding decay is not considered. Elastic scattering of Δ's,

$$\Delta_1 + N_2 \to \Delta_3 + N_4, \quad (12)$$

is also included with a cross section like NN scattering. In the case such processes occur we repeat procedure (4a) until no Δ's are left.

(4b) In case a pion is formed we first follow the trajectory of the pion in an attractive potential given by the nuclear mean field. We follow the pion until it either escapes the target nucleus or reacts with a nucleon in the target,

$$\pi + N \to \Delta. \quad (13)$$

The possibility for reacting depends on the invariant mass M^* of the reaction through the empirical relation for the cross section,

$$\sigma(M^*) = \sigma_{\pi N} \frac{P(M^*)}{P(M_\Delta)}, \quad (14)$$

with $P(M)$ given by Eq. (6) and with $\sigma_{\pi^+ p} = 200$ mb. In case a new Δ is formed we go back to step (4a) to investigate the further story of this Δ. We keep track of all nucleons involved until this stage of the reaction. They are followed out of the target nucleus under point (5). In case the pion escapes, we go to (5) to follow all earlier involved nucleons out of the target nucleus.

(5) When only nucleons are left in the target we follow each nucleon in the mean field, investigating at each time step whether it collides with other nucleons or not. If it collides the momentum is changed correspondingly and propagation is continued. All collisions are performed with nucleons in the local Fermi sea, and collisions are only done if no collision products are Pauli blocked. All nucleons involved in collisions are followed until they escape the target nucleus. No collisions between once collided nucleons are taken into account.

III. SENSITIVITY TO INGREDIENTS IN THE MODEL

To illustrate the sensitivity to the parameters of the model we first look at the division of the events according to types and numbers of particles that we would observe in a realistic detector, in this case the Diogene-Chalut detector at SATURNE [1]. This detector is simulated by allowing ejectile detection at a rectangular area measuring triton particles where p_x/p_z is between $-1°$ and $+4°$, and where p_y/p_z is between $-0.8°$ and $+0.8°$. Charged decay products are measured in angles between 20° and 132° from the beam axis. For pions the kinetic energy should be above 15 MeV whereas the threshold for protons is 35 MeV. We use a ^{3}He beam with kinetic energy of 2 GeV, and we use ^{12}C as our standard choice of target.

The initial step of our model is to calculate where in

[3]Notice that the total cross section for $n\Delta^{++} \to pp$ does not depend on how far the Δ mass is from the $(m_n + m_\pi)$ threshold. The threshold dependence emphasized in Ref. [11] relates only to the ratio of the two inverse cross sections and comes solely from the dependence on distance from the Δ threshold for the cross section for $pp \to n\Delta^{++}$.

the target nucleus the Δ's are formed. This is described in the Appendix. Using realistic density profiles of both projectile and target nucleus and applying an absorptive cross section for the ^{3}He projectile of 3×40 mb, Fig. 1 shows the impact parameter distribution of Δ's formed initially. We notice that in case of a pointlike projectile, the distribution of impacts of successful events equals the distribution of Δ's. In case of a finite-size projectile these two distributions differ, reflecting that the projectile might pass the target at larger impacts where its chance to be absorbed is less, and simultaneously, by its density tail, trigger the formation of Δ's deeply inside the target. In fact the average reaction corresponds to a Δ formed at an impact of 2.8 fm whereas the corresponding projectile pass at impact $b = 3.9$ fm.[4] For the formation of the initial Δ this simplification is partly justified by the forward peaked distribution of the three-momentum transfer **q** (at most 30° from the beam direction), making the extension of the interaction perpendicular to the beam small. Inclusion of finite range effects of the interaction has only been simulated by further extension of the finite size of the projectile. For the same formation cross section (by adjusting the absorption cross section) the effect on the inclusive spectrum and the ratios between yields in the different decay channels is small.

Table I shows the fraction of different event classes. We show several simulations, first for a pointlike projectile, then for a realistic projectile (with root mean square radius equals that of ^{3}He). In both cases we bombard a ^{12}C target with a 2 GeV ^{3}He beam. Then we show how the distributions would look if we used a ^{208}Pb target instead. In these three situations we use parameters for formation of Δ's inside the medium that roughly fits (see later) the inclusive energy transfer (omega) spectra [use $(m_\Delta, \Gamma, m_{\pi^+ + m_n})$ =(1202 MeV,200 MeV,1148 MeV) in Eqs. (6)–(8)]. Furthermore we investigate the possibility to use a *deuteron* beam (absorption cross section of 80 mb) and we display the outcome of a reaction similar to the setup used in a (p,n) experiment [2], where a 830 MeV proton beam was used.

In discussing the relative behavior of (p,p) and (p,π) events, i.e., the ratio $R_{p\pi:pp} = \frac{\text{number of } p\pi \text{ events}}{\text{number of } pp \text{ events}}$, we see that the finite size of the projectile alone makes this ratio increase from 0.088/0.173 to 0.091/0.101. The finite projectile probes a wider range of densities in the target nucleus, thereby enhancing differences in reabsorption. The table finally shows that the ratio $R_{p\pi:pp}$ depends primarily on the extension of the projectile and only little on the size of the target.

From Table II we see from where the different decay channels originate in the target nucleus. Because pions are strongly absorbed in the nuclear medium [Eq. (10)] an event with a pion is typically caused by a Δ formed at low density. Thus the $p + \pi$ channel is connected to an initial Δ formed at significant lower density than the $2p$ channel.

The calculated ratios of event types depend on the modelling of the target nucleus, such as the parameters to describe the mean fields for the Δ and pion propagation and the Fermi motion. In contrast to the sensitivity on these ratios, it appears that the mean values of the ω spectra are fairly independent of mean field potentials and details in the motion of target nucleons. In fact the ω spectra can only be altered significantly by changing the properties of the initially formed Δ.

TABLE I. Calculated distribution of reaction classes. Event classes defined as they would be observed in the Diogene-Chalut detector (experimental result on first line), except for the 830 MeV proton beam (last line, where we model the Japanese detector). We always use medium parameters as given in the text. Notice that medium parameters for proton beam and ^{3}He differ. σ_{abs} is the projectile absorption cross section in mb chosen to fit the measured total cross section, except for the second line where we investigate a point projectile with a strong absorption. The deuteron wave function is modeled by [17], its beam energy equals that of ^{3}He per nucleon, and as form factor we use the ^{3}He form factor.

Event type	None	p	π	(p,p)	(p,π)	(p,p,p)
^{3}He+^{12}C, experiment	0.32	0.26	0.19	0.14	0.07	0.014
^{3}He(point)+^{12}C, $\sigma_{\text{abs}} = 120$	0.311	0.241	0.208	0.077	0.152	0.008
^{3}He(point)+^{12}C, $\sigma_{\text{abs}} = 76$	0.418	0.256	0.160	0.073	0.088	0.006
^{3}He(finite) +^{12} C, $\sigma_{\text{abs}} = 120$	0.351	0.293	0.153	0.101	0.091	0.010
As above but $2\sigma_{N\Delta\to NN}$	0.301	0.319	0.141	0.137	0.089	0.011
^{3}He(finite)+^{208}Pb, $\sigma_{\text{abs}} = 120$	0.325	0.332	0.138	0.115	0.071	0.017
^{2}H(finite)+^{12}C, $\sigma_{\text{abs}} = 80$	0.370	0.317	0.127	0.111	0.065	0.009
p(finite) +^{12} C, $\sigma_{\text{abs}} = 40$	0.258	0.262	0.184	0.082	0.183	0.018

[4]Possible effects from the remaining two projectile nucleons on the Δ are ignored. These effects are partly included in the independently measured form factor. There might however be some additional effects due to the simultaneous presence of both projectile and target matter. Using average trajectories, and modeling the projectile as independent nucleons with a Gaussian density distribution, one can estimate that the average projectile density at the Δ formation point is 0.032 fm^{-3}.

TABLE II. Density (fm^{-3}) at which the event classes are initiated.

Event type	p	π	(p,p)	(p,π)	(p,p,p)	Incl.
^{3}He(point)+^{12}C, $\sigma_{abs}=120$	0.021	0.010	0.023	0.009	0.022	0.016
^{3}He(point)+^{12}C, $\sigma_{abs}=76$	0.033	0.017	0.037	0.011	0.026	0.027
^{3}He(finite)+^{12}C, $\sigma_{abs}=120$	0.055	0.024	0.057	0.017	0.046	0.045
^{3}He(finite)+^{208}Pb, $\sigma_{abs}=120$	0.044	0.016	0.045	0.010	0.035	0.036
^{2}H(finite)+^{12}C, $\sigma_{abs}=80$	0.066	0.033	0.067	0.020	0.057	0.057
p(finite)+^{12}C, $\sigma_{abs}=40$	0.054	0.043	0.068	0.029	0.060	0.051

IV. COMPARISON WITH EXPERIMENT

A. ^{12}C(^{3}He,t) reaction at 2 GeV

In this section we compare in more detail with data from the experiment at SATURNE [1]. In Fig. 2 the calculated formation cross section is compared to the inclusive spectrum integrated over the solid angle in the setup as described above. The cross section for absorption of the ^{3}He or triton particles is taken as 3×40 mb^2 and is not considered a free parameter.

The parametrized form of the elementary cross section ($NN \to N\Delta$) as given in Eq. (5) is normalized to fit the $p(^3\text{He},t)\Delta^{++}$ data [12] and the formation cross section for the ^{12}C target is then calculated as described in Sec. II. Results for three different sets of parameters for the Δ isobar are shown in Fig. 2. The calculated cross section with free Δ parameters ($M_\Delta = 1232$ MeV, $\Gamma = 120$ MeV) is far too small (only 0.66 mb) and the peak in the spectrum is 80 MeV higher in energy than in experiment. Increasing the width to $\Gamma = 200$ MeV gives an increase of the total cross section to 0.77 mb and moves the peak down by about 45 MeV. By furthermore decreasing the Δ mass to $M_\Delta = 1200$ MeV the measured cross section of 1.25 mb is reproduced with a somewhat too narrow Δ peak compared to the data. The changing of the mass of the Δ isobar inside the nucleus can be considered as a crude way to simulate effects from Δ-hole correlations. Interactions based on one-pion exchange are attractive and do lead to a lowering of the energy of Δ-hole states. Detailed microscopic calculations have been performed for both (p,n) and (^{3}He,t) induced Δ excitations [13–15]. Figure 2 illustrates that the steep form factor for the ^{3}He-t system emphasizes the part of the Δ-hole states that is shifted down in energy. [This is in contrast to the (p,n) case as shown in Fig. 5, where the calculated cross section for the three parameter sets are similar.]

Projectile excitation for ^{3}He is not included in this calculation of the cross section as the effect in a cascade picture is completely negligible, because the probability to end up in the ground state of the ejectile (the triton) would be very small.

In Figure 3 calculated energy-transfer spectra for different decay channels are compared to data. The formation cross section is calculated with "medium" parameters (M_Δ=1202 MeV, Γ_Δ= 200 MeV) to come closer to the measured inclusive spectrum. In the upper part (a) of the figure, the decay is calculated with parameters as described in (4a) and (4b), i.e., with the "free" width for pion + nucleon decay, modified by Pauli blocking, plus a width for two-nucleon decay corresponding to the free $N\Delta \to NN$ cross section. The gross features of the data are then reproduced, but we see that increasing by a factor 2 this $N\Delta \to NN$ cross section, as done for the calculations shown in the middle section (b) of the figure, the ratios between the $2p$ and the $(\pi + p)$ channels are much closer to experiment. [The same effect is observed for the (p,n) case given in Fig. 6.] We note that in this calculation three-nucleon absorption is included and it is therefore not this process that can justify our suggested increase of the in-medium cross section by a factor 2. It is seen from Fig. 3 that most of the observed energy shift between the $2p$ and $(\pi + p)$ channels is accounted for, but the experimental ω spectrum for the $2p$ channel stretches much farther down into the dip region between the quasielastic and Δ peak. In the calculations we can identify the origin of the shift between the two channels. At small ω the $(\pi+p)$ decay is hindered by the threshold effect in this channel. The decay width as given by Eq. (7) has a $(p_\pi)^3$ dependence on the c.m. momentum p_π of the pion. The $2p$ decay channel then becomes sensitive to the shifted part of Δ-hole states.

In Fig. 4 the calculated missing mass in the $(\pi + p)$

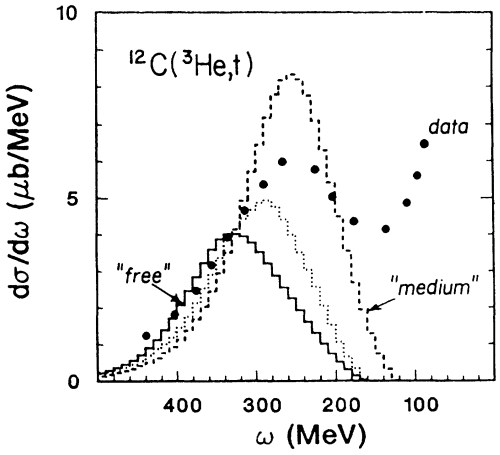

FIG. 2. The inclusive energy-loss spectrum for the ^{12}C(^{3}He,t) reaction at 2 GeV [1] is compared to the calculated Δ-formation cross section into the same solid angle. The cross section for absorption of the ^{3}He or triton particles is taken as 3×40 mb^2. The solid drawn line corresponds to $M_\Delta = 1232$ MeV, $\Gamma = 120$ MeV, the dotted curve to $\Gamma = 200$ MeV, and the dashed curve to $M_\Delta = 1202$ MeV, $\Gamma = 200$ MeV.

channel is compared to data. It is seen that the curve calculated with "free" parameters for the formation cross section does not agree with the data for the carbon target, but with the data from the proton target. The curves with "medium" parameters for the formation cross section describe the data very well, and a change of the $\Delta N \rightarrow NN$ in-medium cross section has a small effect on the missing mass spectrum. The conclusion from this would be that the $(\pi+p)$ decay channel does not carry information on medium effects other than is already in the formation cross section, i.e., in the inclusive spectrum.

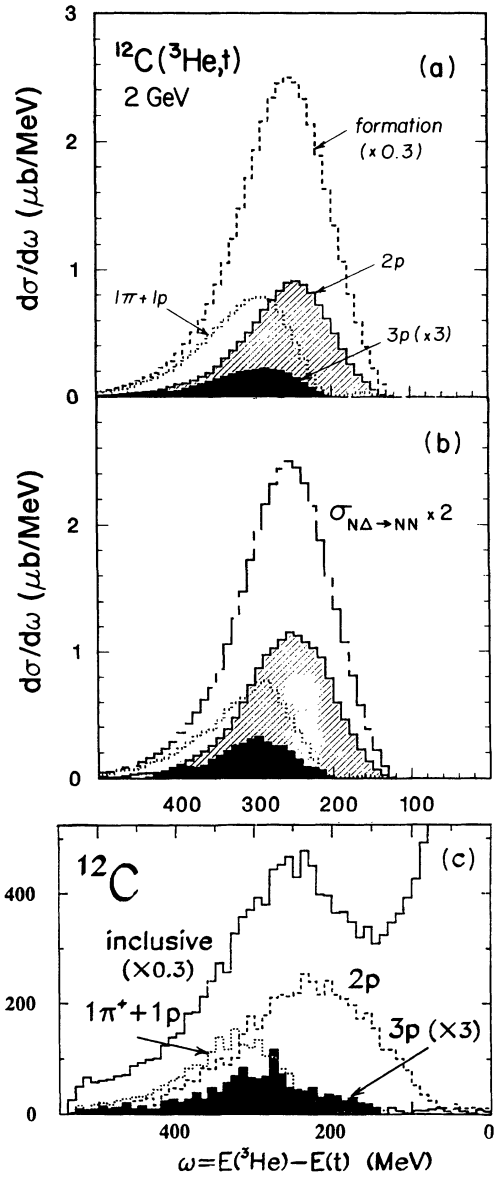

FIG. 3. Calculated energy-transfer spectra for different decay channels are compared to data. The formation cross section is calculated with "medium" parameters (M_Δ = 1202 MeV, Γ_Δ = 200 MeV) (see Fig. 2). In the upper part (a) of the figure, the decay is calculated with "free" parameters. In (b) the $N\Delta \rightarrow NN$ cross section is increased a factor of 2. The data from Ref. [1] are shown in (c).

B. $^{12}C(p,n)$ reaction at 830 MeV

A comparison with the (p,n) decay data from the KEK experiment [2] is also very instructive. The acceptance in angle and energy is similar to the SATURNE experiment. In Fig. 5 the measured inclusive spectrum is compared to the calculated formation cross section for the three sets of Δ parameters used in Fig. 2 for the (^{3}He,t) data.

We see that the contribution from the shifted part of the Δ peak needs to be much smaller in the (p,n) case to fit the data. In the (^{3}He,t) case the steep form factor enhances this shifted part.

For the (p,n) case we furthermore include the projectile excitation in the calculated spectra. It is noted that this has little influence on the final outcome.

In Fig. 6 calculated energy-transfer spectra for three

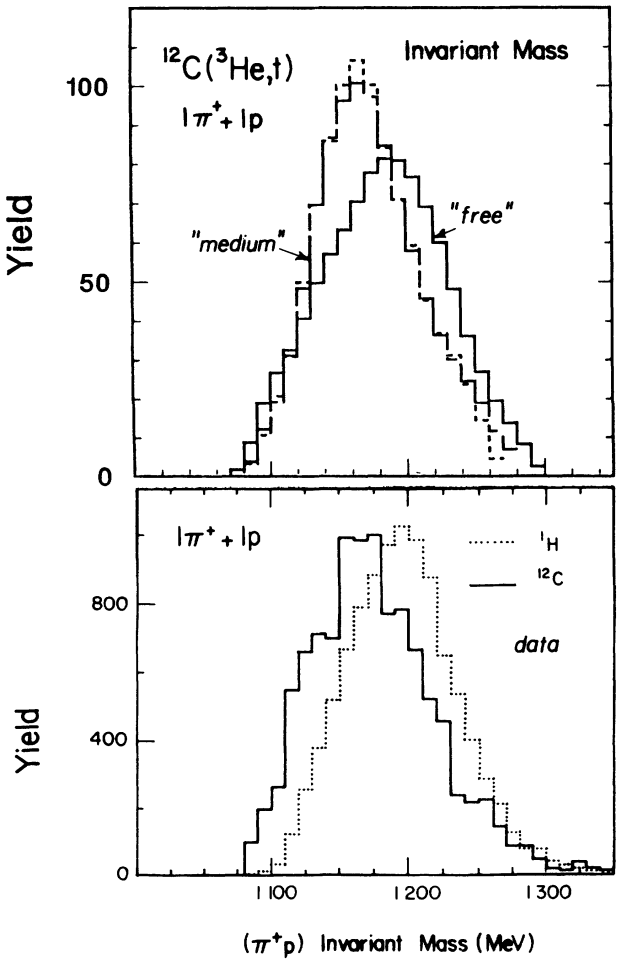

FIG. 4. The calculated missing mass in the $(\pi + p)$ channel is compared to data (lower part) [1] for ^{12}C and proton targets. The solid drawn curve corresponds to a formation cross section calculated with "free" parameters and is seen not to agree with the data for the carbon target, but with the proton data. The curves with "medium" parameters for the formation cross section describe the data quite well, and a change of the $\Delta N \rightarrow NN$ in-medium cross section has a small effect on the missing mass spectrum.

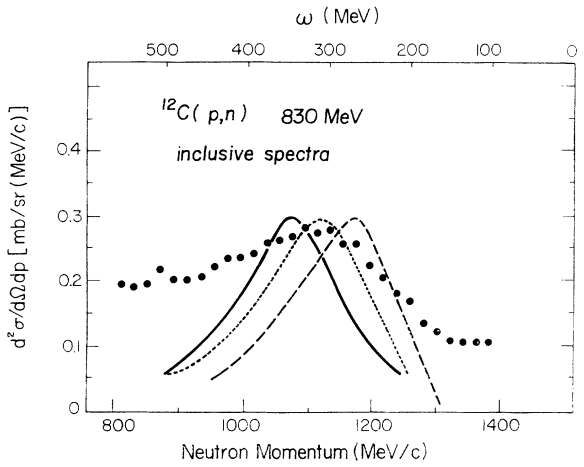

FIG. 5. The measured inclusive spectrum from the KEK experiment [2] is compared to the calculated formation cross section for the three sets of Δ parameters used in Fig. 2 for the (^{3}He,t) data. The solid drawn line corresponds to M_Δ = 1232 MeV, Γ = 120 MeV, the dotted curve to Γ = 200 MeV, and the dashed curve to M_Δ = 1202 MeV, Γ = 200 MeV. An absorption cross section of 40 mb is used.

decay channels are compared to data. The formation cross section is in this case calculated with Δ parameters M_Δ = 1232 MeV, Γ = 200 MeV, i.e., only the width is increased. In the middle part of the figure the $\Delta N \rightarrow NN$ cross section was increased a factor of 2 as for the (^{3}He,t) case in Fig. 3(b).

This gives a better agreement with the experimental data on the yield in the $2p$ channel. We note that we have not attempted to fit the formation cross section. This could have been done by taking the formation cross section as a sum of contributions with different parameters for the Δ. This would not at all be unreasonable since this is what does come out of the microscopic calculations. The interactions, e.g., in the spin-longitudinal and spin-transverse channels are taken to be different and this leads to different energies of the Δ-hole states in the different spin channels. If such a fit is enforced by combining different Δ-parameter sets a very reasonable agreement is obtained with the data from Fig. 6 [except for the low-energy part of the $2p$ spectrum, as in the (^{3}He,t) case].

In Fig. 7 calculated invariant mass spectra for the ($\pi^+ + p$) decay channel are compared to data. We see that this quantity is not very sensitive to the model parameters.

C. $2p$ decay channel

The $2p$ decay is an important channel in both the (p,n) and (^{3}He,t) reactions. In Figs. 8, 9, and 10 calculated spectra are compared to data from the (^{3}He,t) induced decay experiment. In Fig. 8 the measured relative angles in the laboratory system between the two protons are compared to cascade calculations. An excellent agreement is obtained. The calculated distribution is however not sensitive to model parameters. The relative angle integrated over $\mathbf{q}$ and ω is mostly determined by phase space and carries little information.

In Fig. 9 the calculated missing energies for different parameter sets are compared and also this quantity is not

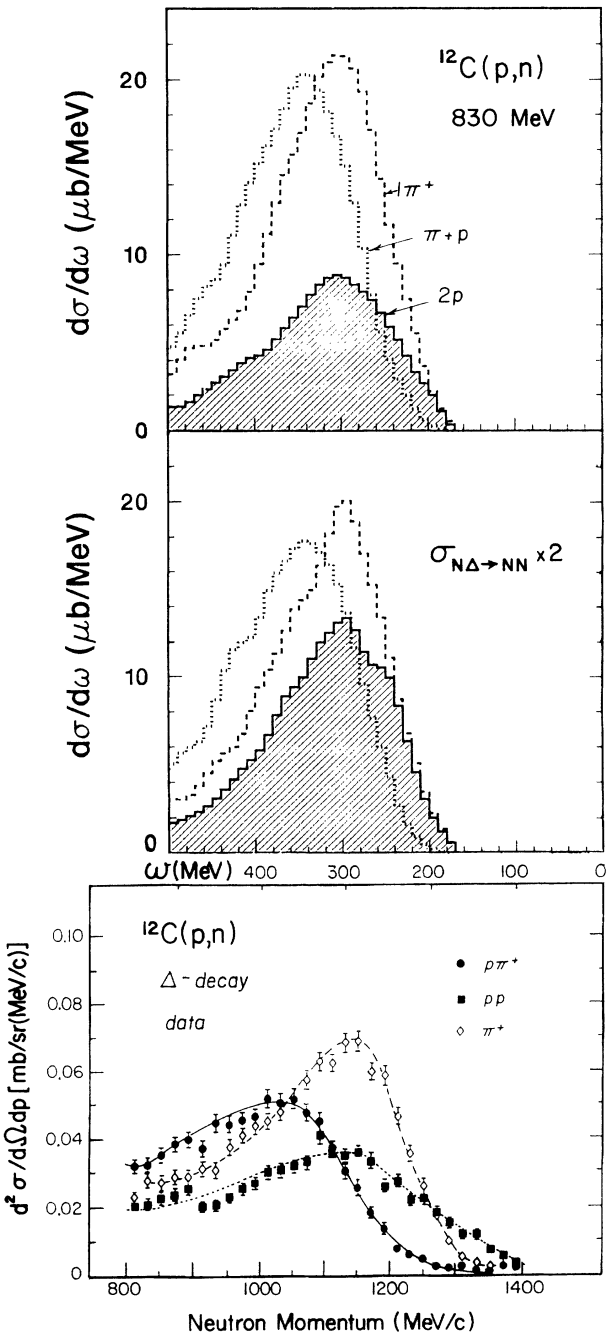

FIG. 6. Calculated energy-transfer spectra for three decay channels are compared to data. The formation cross section is in this case calculated with Δ parameters M_Δ = 1232 MeV, Γ = 200 MeV (the middle curve in Fig. 5); i.e., only the width is increased. In the middle part of the figure the $\Delta N \rightarrow NN$ cross section is increased a factor of 2 as for the (^{3}He,t) case in Fig. 3.

very sensitive to these parameters. In Fig. 10 calculated spectra are compared to data for ^{12}C and ^{208}Pb and it is seen that the measured spectrum peaks at lower missing energy, i.e., lower excitation energy in the final nucleus. Two effects explain most of the discrepancy. The large two-nucleon separation energies for both the ^{12}C and ^{208}Pb nuclei (relative to average as implicitly assumed in the model) give a downward shift. The other effect is related to the low-energy part of the $2p$-energy-transfer spectrum, as given in Fig. 3, and not accounted for in the cascade model. This part has a low excitation energy or small missing energy and it therefore contributes to the yield in Fig. 10 not described in the simulations.

Also shown in Fig. 10 are data from the $(\pi^+, 2p)$ reaction on three different targets [16] to demonstrate the dramatic difference to the (^{3}He,t $2p$) reactions. The latter could be thought of as absorption of an off-shell pion and we see that the cascade simulation does quite well in explaining the data. Both reactions are certainly surface reactions and it would be interesting to do a cascade simulation of real pion absorption to see whether the missing energy spectra could be described as demonstrated here for the (^{3}He,t $2p$) reaction. Published cascade calculations of pion absorption [19] did not consider this particular channel, where data only recently have become available.

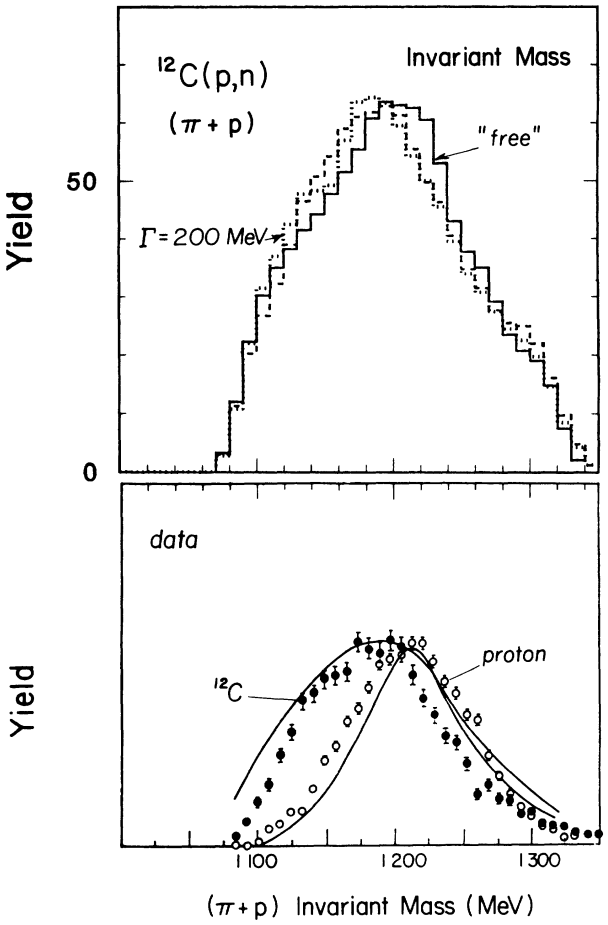

FIG. 7. Upper part of figure: Calculated invariant mass spectra for the $(\pi^+ + p)$ decay channel are shown with two parameter sets for the formation cross section: "free," solid drawn curve; $M_\Delta = 1232$ MeV, $\Gamma = 200$ MeV, dashed curves; short dashed, the $\Delta N \rightarrow NN$ cross section is increased. In the lower part of the figure, data is compared to calculated spectra. For ^{12}C the long dashed curve from the upper part of the figure is used.

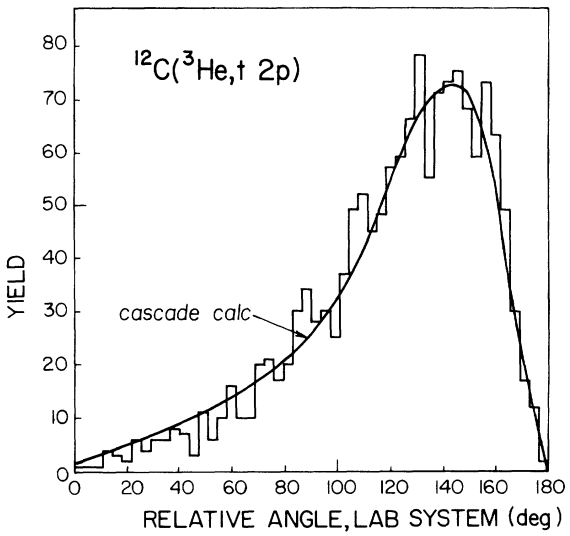

FIG. 8. The measured relative angle in the laboratory system between the two protons are compared to calculations with "medium" parameters for the formation cross section. The calculated distribution is however not sensitive to model parameters.

D. Coherent pions

The decay experiment at SATURNE has also presented evidence for coherent pions [18]. The signals for such events are shown in Figs. 11 and 12. The cross

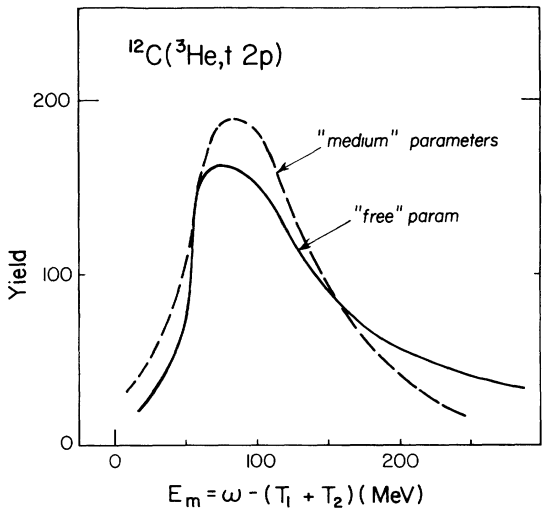

FIG. 9. The calculated missing energy for the $2p$ decay channel for different parameter sets are compared.

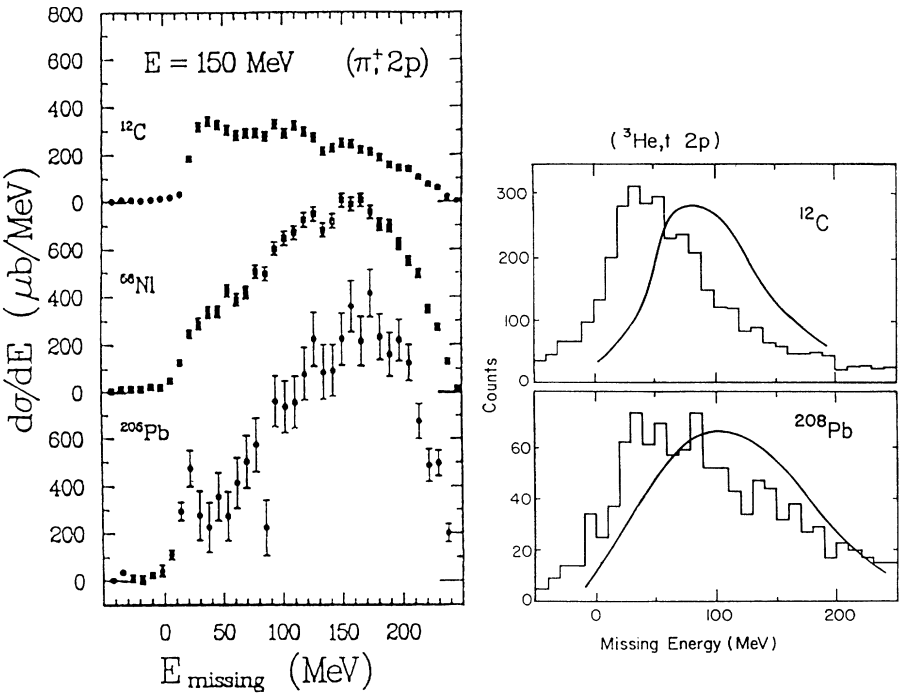

FIG. 10. Calculated missing energy spectra for the (^{3}He,t 2p) reaction with "medium" parameters are compared to data for ^{12}C and ^{208}Pb. Also shown are data from the (π^+,2p) reaction on three different targets [16] to demonstrate the dramatic difference to the (^{3}He,t 2p) reactions.

section for single pion events where the target nucleus is left in the g.s. or a bound state is far larger than phase space dictates and furthermore a strong angular correlation is observed between the direction of the transferred momentum and that of a pion, where the final state in the target is a bound state.

In the cascade simulations of the experiment single π^+ events result from ($\pi^+ + N$) decays, in which the nucleon is not detected either because it is a neutron, or a proton outside the angular acceptance of the detector — or with an energy below threshold. The probability for leaving the target nucleus in a bound state after emission of a single pion is extremely small. This is demonstrated in Fig. 11, where the calculated missing mass spectrum for single pion events is compared to data. It is seen that the calculated spectrum has a very small yield below $\sim$ 20 MeV above the g.s mass of the target nucleus. This is in contrast to the measured spectrum where a significant part corresponds to bound states. We note that the experimental resolution in missing mass is around 25 MeV [full width at half maximum (FWHM)] and the calculated spectrum has been folded with the same resolution.

In Fig. 12 the measured angular correlation between the direction of the transferred momentum and that of a pion from single-pion events is shown with different gates on the missing mass. A very sharp peaking for small relative angles is observed for events where the missing mass spectrum corresponds to bound states. Also shown in the figure are calculated angular correlations for different gates in the calculated missing mass spectrum. We see a much less pronounced peaking at small relative angles. In the simulation the peaking is a phase space effect.

In conclusion, the coherent pions are not treated in the cascade model, but the simulations are still useful in understanding phase space effects. We note that the contribution from the coherent pions is experimentally found to contribute with only about 6% to the inclusive energy-transfer spectrum [18].

V. CONCLUSION

We have presented results of cascade simulation of Δ formation and decay initiated in the charge-exchange re-

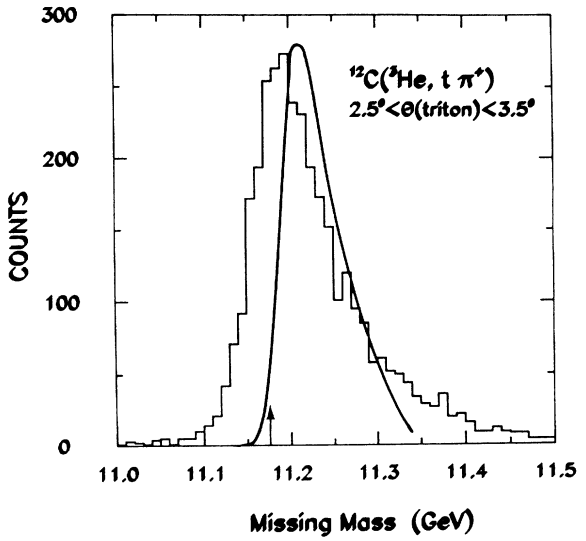

FIG. 11. The measured missing mass spectrum for single-pion events are compared to calculation. The resolution is around 25 MeV (FWHM) and the calculated curve has been folded accordingly. The arrow shows the g.s. mass for ^{12}C and yield below is due to the finite resolution. The missing mass for ^{11}C(g.s.) + n is 11.194 GeV and for ^{11}B(g.s.) + p is 11.191 GeV.

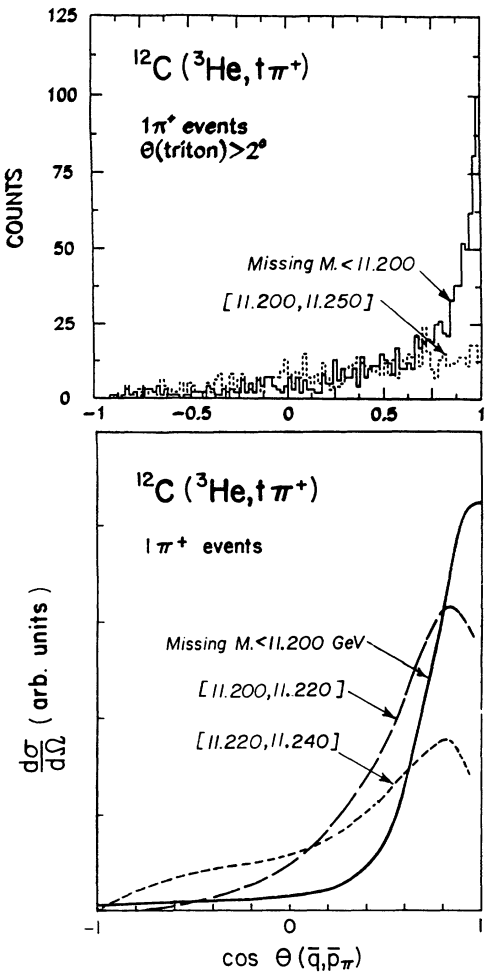

FIG. 12. The measured angular correlation between the transferred momentum **q** and the momentum of pions with different conditions on the missing mass for $1\pi^+$ events with a triton angle larger than 2° is compared to calculated angular correlations (lower part of the figure).

actions (p,n) and (^{3}He,t). The Δ isobars are in both these reactions formed in the surface region since only events are considered where fast forward ejectiles are detected. The formation process corresponds to quasifree Δ formation, but we find that free parameters for the Δ properties do not reproduce the measured inclusive spectrum. This is especially so for the (^{3}He,t) case where the steep form factor enhances the low energy-transfer part of the inclusive spectrum. This is consistent with the literature on the origin of the shift of the Δ peak in charge-exchange reactions.

By changing the mass and width of the Δ isobar in the formation process a better agreement with the inclusive spectrum is enforced and the gross features of the decay is then reproduced. We find that by increasing the in-medium $N\Delta \rightarrow NN$ cross section relative to the "free" value, the measured ratio of yields in the $(\pi + p)$ and $2p$ decay channels are better reproduced. We note however that this ratio does depend on two-particle correlation effects, which are treated very primitively in this approach.

Two effects in the decay are not accounted for by the simulations. The energy-transfer spectrum in the $2p$ channel stretches far into the dip region. This effect is related to the shift in the inclusive spectrum, but the decay experiment gives much more detailed information on the origin of the shift. Also the coherent pions are not accounted for in these calculations. This coherence is a truly collective effect which is not part of this model.

In experiments like the ones referred to in this paper, where very complex events are recorded, we have seen that the real important and interesting information often only appears after multidimensional gating. Here the cascade simulations are extremely useful to understand "trivial" correlations from phase space and detector acceptance effects.

ACKNOWLEDGMENTS

We would especially like to thank V. Dmitriev, M. Ichimura, T. Sams, W. Weise, and V. Zelevinski for stimulating discussions during the course of this work. K.S. thanks the Carlsberg Foundation for financial support.

APPENDIX: WHERE THE Δ ISOBAR IS FORMED

We here describe how the distribution of initially formed Δ isobars is generated. In principle we could run the cascade program directly, by careful calculation of the projectile-ejectile trajectory through the target nucleus, thus sampling events where one and only one Δ was formed during the passage. When doing this, most of the computer time is used on events, where either no Δ was formed, or where the projectile scattered more than once with the target nucleons. Therefore we instead as an initial step calculate the spatial distribution of successfully formed Δ resonances, under the condition of one and only one interaction between the projectile and the target.

For completeness we describe two such approaches, differing in modeling of the projectile density distribution. In both cases we explicitly consider a ^{3}He nucleus, but generalizations are straightforward. In both cases we consider straight line geometry only and include events, where the projectile interacts once with a target nucleon. The cross section for such an interaction forming a Δ is denoted σ_Δ. The total cross section for a reaction between the projectile and a target nucleon is denoted $\sigma_{\rm abs}$. As we only allow for one interaction between projectile and target, the distribution of events will be symmetric with respect to $z \rightarrow -z$ where $z = 0$ is the target center and the z-axis parallel to the beam.

In model A the density distribution of the projectile is immediately (before propagation through the target) converted into the positions of three pointlike projectile particles, each carrying their fraction of the projectile cross section for eventual interactions.

In model B the average projectile density profile is carried through the target nucleus, allowing for interactions everywhere with probabilities given solely by the overlap

of the average projectile profile with the target. Thus model B ignores correlations between projectile nucleons that in the successful events come from the condition that none of them scatter on any target nucleons. On the other hand, model B is faster to implement, allows for generalizations that takes into account finite range of the interactions, and does not demand the independent Monte Carlo sampling of model A.

It is noted that predictions of model A and model B only differ slightly for the studied ^{3}He projectile. Especially when the absorption cross section for the projectile is adjusted to fit the observed cross section, there is no measurable consequence. The calculations presented in the paper corresponds to model B.

Model A

We now describe a Monte Carlo sampling for both the total cross section for Δ formation and for the spatial distribution of initially formed Δ isobars. The cross section for the projectile to make one successful reaction when its center of mass has an impact parameter $[b, b+db]$ is

$$F_{\rm hit}(b)db = 2\pi b\, db \int\int\int d^2x_1 d^2x_2 d^2x_3 \quad P(\mathbf{x}_1,\mathbf{x}_2,\mathbf{x}_3) R_\Delta(\mathbf{x}_1+\mathbf{b},\mathbf{x}_2+\mathbf{b},\mathbf{x}_3+\mathbf{b})\; A_{\rm abs}(\mathbf{x}_1+\mathbf{b},\mathbf{x}_2+\mathbf{b},\mathbf{x}_3+\mathbf{b}). \tag{A1}$$

Here the planar (perpendicular to the beam) probability distribution of the three projectile nucleons in its center of mass frame ($\mathbf{x}_1+\mathbf{x}_2+\mathbf{x}_3=0$) is given by

$$P(\mathbf{x}_1,\mathbf{x}_2,\mathbf{x}_3) = \frac{\rho_{\rm proj}(\mathbf{x}_1,\mathbf{x}_2,\mathbf{x}_3)}{\int d^2x_1 d^2x_2 d^2x_3 \rho_{\rm proj}(\mathbf{x}_1,\mathbf{x}_2,\mathbf{x}_3)}, \tag{A2}$$

where $\rho_{\rm proj}$ is the projectile density profile projected to a plane perpendicular to the beam. Given the initial positions of the projectile nucleons $(\mathbf{y}_1,\mathbf{y}_2,\mathbf{y}_3)$= $(\mathbf{x}_1+\mathbf{b},\mathbf{x}_2+\mathbf{b},\mathbf{x}_3+\mathbf{b})$ the probability that one of these reacts successfully is (it must be a proton)

$$R_\Delta(\mathbf{y}_1,\mathbf{y}_2,\mathbf{y}_3) = \sum_{i\in \text{proj proton}} \sigma_\Delta^n \int_{-\infty}^{\infty} dz \rho_{\rm targ}(\mathbf{y}_i+\mathbf{z}), \tag{A3}$$

whereas the probability that all the projectile nucleons pass the target nucleus without absorbtions is given by

$$A_{\rm abs}(\mathbf{y}_1,\mathbf{y}_2,\mathbf{y}_3) = \exp\left(-\sum_{i\in\text{projectile}} \sigma_{\rm abs}^n \int_{-\infty}^{\infty} dz \rho_{\rm targ}(\mathbf{y}_i+\mathbf{z})\right). \tag{A4}$$

In these formulas the total projectile cross section is divided equally on each of the possible projectile nucleons, e.g., is the total projectile absorbtion cross section $\sigma_{\rm abs}$ given as a sum of equal independent projectile nucleon scattering cross sections $\sigma_{\rm abs}^n$. For each b then $F_{\rm hit}(b)$ is calculated by Monte Carlo sampling of the positions of the projectile nucleons in accordance with the density distribution. For each selected set of initial positions perpendicular to the beam, we calculate the integrals in $F_{\rm hit}$ along the beam, thus obtaining the contribution to the cross section of this particular choice of projectile nucleon positions. Averaging over a big number of initial projectile nucleon positions, we obtain $F_{\rm hit}(b)$. The total cross section is

$$\sigma_{\rm total} = \int db F_{\rm hit}(b). \tag{A5}$$

Similarly, the spatial distribution of successfully formed Δ can be obtained from Monte Carlo sampling of projectile nucleon positions:

$$P(b',z)db'dz = \sum_{i\in\text{projectile}} 2\pi b\, \delta(|\mathbf{x}_i+\mathbf{b}|-b')\; \rho_{\rm targ}[\mathbf{x}_i+\mathbf{b}+(0,0,z)] A_{\rm abs}(\mathbf{x}_1+\mathbf{b},\mathbf{x}_2+\mathbf{b},\mathbf{x}_3+\mathbf{b})\; P(\mathbf{x}_1,\mathbf{x}_2,\mathbf{x}_3)\; db'dz, \tag{A6}$$

where b is the c.m. impact of the projectile and $\mathbf{x}_1,\mathbf{x}_2,\mathbf{x}_3$ are the c.m. coordinates of the projectile nucleons perpendicular to the beam.

Model B

We here describe the calculation of the spatial distribution of Δ isobars formed from propagation of the average projectile density profile the whole way through the target nucleus.

Suppose that the center of mass of the projectile is at position $(b,0,z)$. The chance that a reaction happens between one nucleon of the projectile and one nucleon on the target is now given by the "effective density" at $(b,0,z)=\mathbf{b}+\mathbf{z}$:

$$G(b,z) = \frac{\int d^3x\, \rho_{\rm proj}(\mathbf{x})\, \rho_{\rm targ}(\mathbf{b}+\mathbf{x}+\mathbf{z})}{\int d^3x\, \rho_{\rm proj}(\mathbf{x})}. \quad \text{(A7)}$$

The Δ-formation probability for a projectile trajectory at impact parameter b is therefore

$$R_\Delta(b) = \sigma_\Delta \int_{-\infty}^{\infty} dz\, G(b,z). \quad \text{(A8)}$$

The probability for not being absorbed is

$$A_{\rm abs}(b) = \exp\left(-\sigma_{\rm abs} \int_{-\infty}^{\infty} dz\, G(b,z)\right), \quad \text{(A9)}$$

and the cross section to form one Δ without absorption at impact $[b, b+db]$ is

$$F_{\rm hit}(b)db = 2\pi\, b\, db\; R_\Delta(b)\; A_{\rm abs}(b). \quad \text{(A10)}$$

The total cross section for formation of a single Δ is given by Eq. (A5).

Selecting a ^{3}He projectile with $\sigma_{\rm abs} = 120$ mb, a Gaussian density profile with rms= 1.75 fm, and using "medium" parameters for Δ-isobar formation, we obtain $\sigma_{\rm total}(^{12}{\rm C}) = 1.4$ mb. For comparison, if we set the extension of the projectile equal to zero, we get $\sigma_{\rm total} = 0.9$ mb with the same parameters for absorption and Δ formation. Experimentally the reaction ^{12}C(He,t)X, Δ has a cross section of 1.25 mb, whereas $\sigma(p({\rm He},t)n) = 0.53$ mb for 2 GeV beam energy.

Given that the projectile center of mass is at position $\mathbf{b}+\mathbf{z} = (b,0,z)$ when a Δ is formed we can calculate the probability that the reaction occurred at impact parameter between b' and $b'+db'$ and at z' between z' and $z'+dz'$:

$$P_{\rm cond}(b',z' \mid b,z) = b'\, db'\, dz' \int d\theta\, \rho_{\rm targ}[\mathbf{b}'(\theta)+\mathbf{z}']\, \rho_{\rm proj}\{\mathbf{b}+\mathbf{z}-[\mathbf{b}'(\theta)+\mathbf{z}']\}, \quad \text{(A11)}$$

where the integration is over all angles of $\mathbf{b}'$ perpendicular to the beam. The chance for a Δ formed at position z, b' is

$$P(b',z')\, db'\, dz' = \sigma_\Delta \int db\, dz\, P_{\rm cond}(b',z' \mid b,z)\, G(b,z)\, 2\pi b A_{\rm abs}(b). \quad \text{(A12)}$$

We note that for a very narrow projectile $G(b,z)$ equals the target density profile and $P_{\rm cond}$ degenerates into $b'\delta(b-b')\delta(z-z')$. Thus, in that case, the probability to have a successful reaction in (b',z') equals the product of the reaction probability at (b',z') with the probability that nothing else happens earlier or later.

Finally we note that for a projectile with a Gaussian density profile (as ^{3}He) $\rho_{\rm proj}(x,y,z) = \rho_{\rm proj}(x)$, $\rho_{\rm proj}(y)$, $\rho_{\rm proj}(z)$ and calculations can be simplified by integrating only coordinates perpendicular to the beam (set $z' = z$ in the above equations).

[1] T. Hennino, B. Ramstein, D. Bachelier, H. G. Bohlen, J. L. Boyard, C. Ellegaard, C. Gaarde, J. Gosset, J. C. Jourdain, J. S. Larsen, M. C. Lemaire, D. L'Hôte, H. P. Morsch, M. Österlund, J. Poitou, P. Radvanyi, M. Roy-Stephan, T. Sams, K. Sneppen, O. Valette, and P. Zupranski, Phys. Lett. B **283**, 42 (1992).

[2] J. Chiba, T. Kobayashi, T. Nagae, I. Arai, N. Kato, H. Kitayama, A. Manabe, M. Tanaka, K. Tomizawa, D. Beatty, G. Edwards, G. Glasshauser, G. J. Kumbarzki, R. D. Ransome, and F. T. Baker, Phys. Rev. Lett. **67**, 1982 (1991).

[3] J. Cugnon *et al.*, Nucl. Phys. **A352**, 505 (1981); **A379**, 553 (1982); **A489**, 781 (1988).

[4] G. F. Bertsch and S. Das Gupta, Phys. Rep. **160**, 189 (1988).

[5] C. Gregoire, B. Remaud, F. Sebille, L. Vinet, and Y. Raffray, Nucl. Phys. **A465**, 317 (1987); **A468**, 321 (1987); Phys. Lett. B **180**, 198 (1986); **186**, 14 (1987).

[6] U. Mosel, Annu. Rev. Nucl. Part. Sci. **41**, 29 (1991), and references therein.

[7] Gy. Wolf *et al.*, Nucl. Phys. **A517**, 615 (1990); **A545**, 139c (1992).

[8] C. Gaarde, Annu. Rev. Nucl. Part. Sci. **41**, 187 (1991).

[9] V. Dmitriev, O. Sushkov, and C. Gaarde, Nucl. Phys. **A459**, 503 (1986).

[10] A. B. Wicklund *et al.*, Phys. Rev. D **34**, 19 (1986); **35**, 2670 (1987).

[11] P. Danielewicz and G. F. Bertsch, Nucl. Phys. **A533**, 712 (1991).

[12] C. Ellegaard, C. Gaarde, J. S. Larsen, V. Dmitriev, O. Sushkov, C. Goodman, I. Bergqvist, A. Brockstedt, L. Carlén, P. Ekström, M. Bedjidian, D. Contardo, J. Y. Grossiord, A. Guichard, R. Haroutunian, J. R. Pizzi, D. Bachelier, J. L. Boyard, T. Hennino, M. Roy-Stephan, M. Boivin, and P. Radvanyi, Phys. Lett. **154B**, 110 (1985).

[13] T. Udagawa, S. W. Hong, and F. Osterfeld, Phys. Lett. B **245**, 1 (1990).

[14] J. Delorme and P. A. M. Guichon, Phys. Lett. B **263**, 157 (1991).

[15] V. Dmitriev, Phys. Rev. C **48**, 357 (1993).

[16] R. D. Ransome, C. L. Morris, V. R. Cupps, R. W. Fergerson, J. A. McGill, D. L. Watson, J. D. Zumbro, B. G. Ritchie, J. R. Comfort, J. R. Tinsley, R. A. Loveman, S. Dawson, A. Green, P. C. Gugelot, and C. Fred Moore, Phys. Rev. C **45**, R509 (1992).

[17] H. Lacombe *et al.*, Phys. Lett. **101B**, 139 (1981).

[18] T. Hennino, B. Ramstein, D. Bachelier, J. L. Boyard, C. Ellegaard, C. Gaarde, J. Gosset, J. C. Jourdain, J. S. Larsen, M. C. Lemaire, D. L'Hôte, H. P. Morsch, M. Österlund, J. Poitou, P. Radvanyi, S. Rousteau, M. Roy-Stephan, T. Sams, and P. Zupranski, Phys. Lett. B **303**, 236 (1993).

[19] Z. Fraenkel, E. Piasetzky, and G. Kalbermann, Phys. Rev. C **26**, 1618 (1982).